Available online at www.sciencedirect.com
ScienceDirect
Tetrahedron
Tetrahedron 63 (2007) 5832–5838

Enhanced selectivity for inhibition of analog-sensitive protein kinases through scaffold optimization

Chao Zhang[a] and Kevan M. Shokat[a,b,*]

[a]*Howard Hughes Medical Institute and Department of Cellular and Molecular Pharmacology, University of California, San Francisco, CA 94143, USA*
[b]*Department of Chemistry, University of California, Berkeley, CA 94720, USA*

Received 17 January 2007; revised 20 February 2007; accepted 21 February 2007
Available online 24 February 2007

Abstract—The ability to inhibit any protein kinase of interest with a small molecule is enabled by a combination of genetics and chemistry. Genetics is used to modify the active site of a single kinase to render it distinct from all naturally occurring kinases. Next, organic synthesis is used to develop a small molecule, which does not bind to wild-type kinases but is a potent inhibitor of the engineered kinase. This approach, termed chemical genetics, has been used to generate highly potent mutant kinase-specific inhibitors based on a pyrazolopyrimidine scaffold. Here, we asked if the selectivity of the resulting pyrazolopyrimidines could be improved, as they inhibit several wild-type kinases with low-micromolar IC_{50} values. Our approach to improve the selectivity of allele-specific inhibitors was to explore a second kinase inhibitor scaffold. A series of 6,9-disubstituted purines was designed, synthesized, and evaluated for inhibitory activity against several kinases in vitro and in vivo. Several purines proved to be potent inhibitors against the analog-sensitive kinases and exhibited greater selectivity than the existing pyrazolopyrimidines.
© 2007 Elsevier Ltd. All rights reserved.

1. Introduction

Potent and selective inhibitors of protein kinases are valuable tools for probing the cellular functions of kinases.[1,2] However, due to the large number of protein kinases in a cell and their highly homologous active sites, it has proven difficult to find specific inhibitors for individual kinases.[2,3] Our laboratory has developed a chemical approach, which employs genetics to circumvent the specificity problem associated with conventional small-molecule inhibitors of protein kinases.[4,5] The approach exploits a conserved, large hydrophobic residue in the kinase active site (termed the gatekeeper),[6] which makes direct contact with the N^6 amino group of ATP. When this residue is mutated from the naturally occurring bulky residue (methionine, leucine, phenylalanine, threonine, etc.) to glycine or alanine, a novel pocket not found in any *w*ild-*t*ype (*WT*) kinase is created within the kinase of interest. Such engineered kinases, termed *a*nalog-*s*ensitive (*as*) alleles, can thus be potently targeted by inhibitor analogs that contain substituents which occupy this enlarged ATP binding pocket and are occluded from binding to *WT* kinases because they lack the additional pocket.

The utility of an inhibitor, which specifically targets a non-naturally occurring protein kinase is only realized when the *WT* kinase can be replaced with the engineered form in cells or animals. Advances in genetics allow for precise introduction of a single mutation in many single-cell eukaryotes such as the budding yeast with ease. Consequently, the chemical genetic approach has been extensively applied to the study of various yeast kinases enabling selective pharmacological blockage of these kinases for the first time.[7] Analogous genetic manipulation in higher eukaryotes is technically much more challenging and thus represents a significant barrier to the use of chemical genetics to study mammalian protein kinases. Despite the technical barrier, genetically engineered mouse models have been created, which carry an *as* allele in place of the *WT* form for a number of protein kinases allowing for the first in vivo assessment of the effects of a mono-specific protein kinase inhibitor.[8,9] While requiring the extra effort of genetic manipulation compared to traditional pharmacology, chemical genetics allows for a critical control experiment, which addresses the target selectivity of a pharmacological agent that is frequently a major question facing protein kinase inhibitors. An isogeneic *WT* control animal or cell can be treated with the *as* specific kinase inhibitor in parallel to the cell or animal which carries the mutant *as* kinase, thus providing an assessment of any 'off-target' effects of the allele-specific inhibitor.

Keywords: Chemical genetics; Protein kinase inhibitor; Purine scaffold.
* Corresponding author. Tel.: +1 415 514 0472; fax: +1 415 514 0822; e-mail: shokat@cmp.ucsf.edu

0040–4020/$ - see front matter © 2007 Elsevier Ltd. All rights reserved.
doi:10.1016/j.tet.2007.02.089

We initially designed and synthesized a small panel of analogs based on the pyrazolopyrimidine scaffold [exemplified by PP1 (Fig. 1A),[10] a nonselective kinase inhibitor], and showed that some PP1 analogs potently inhibit the engineered kinases.[4,5] However, PP1 analogs still affect certain *WT* kinases such as v-Src and Fyn. For example, 1NA-PP1, one of the most effective allele-specific inhibitors discovered so far, inhibits *WT* v-Src with an IC_{50} of 1 μM (Table 1), suggesting that it could inhibit kinases like v-Src in the cell when used at mid-micromolar or higher concentrations. This has restricted the use of PP1-derived inhibitors to relatively low concentrations. To overcome this limitation, we sought to develop allele-specific kinase inhibitors with improved selectivity over the existing PP1 analogs.

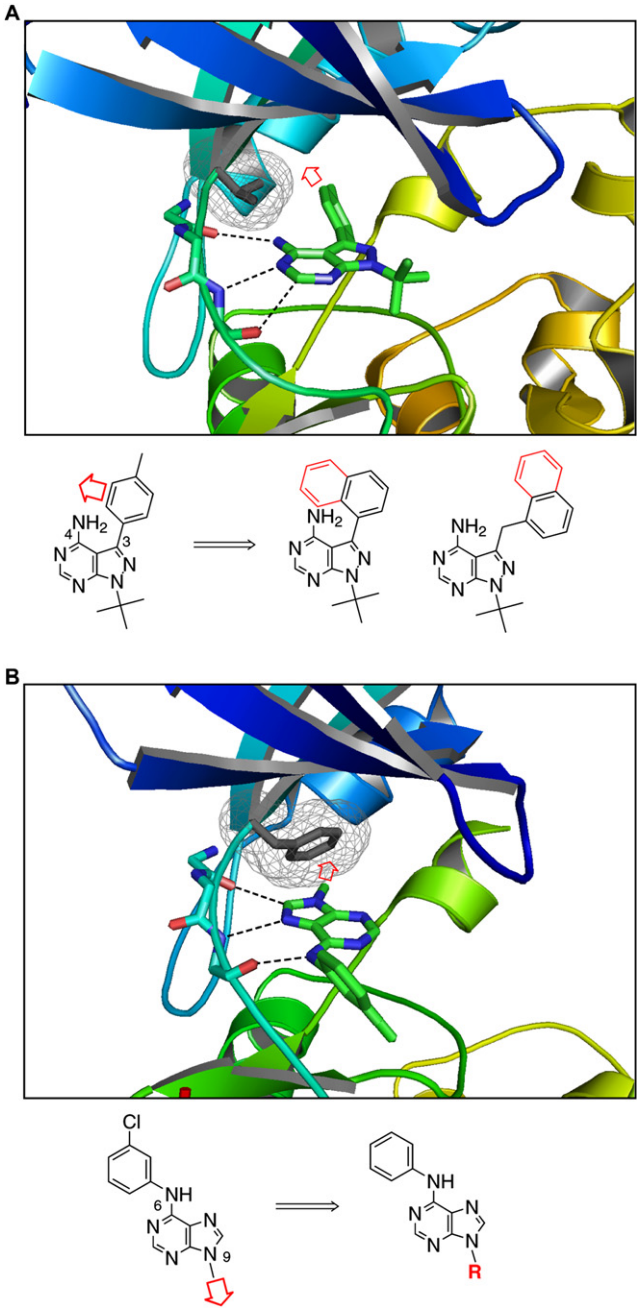

Figure 1. (A) Crystal structure of Hck–PP1 complex at the top and the structures of PP1, 1NM-PP1, and 1NA-PP1 at the bottom. The gatekeeper residue (Thr338) in Hck is highlighted gray with meshed surface and the H-bonds between PP1 and the kinase hinge region are shown in dashed line. The red arrow indicates the point and direction of derivatization on PP1 to generate allele-specific kinase inhibitors. (B) Crystal structure of CDK2–PVA (a purvalanol analog) complex at the top and the structures of PVA and its N9-modified derivatives at the bottom. The gatekeeper residue (Phe80) in CDK2 is highlighted gray with meshed surface and the hydrogen bonds between PVB and the kinase hinge region are shown in dashed line. The red arrow indicates the point and direction of derivatization on PVA to generate allele-specific inhibitors for protein kinases.

In principle, the challenge of improving allele specificity can be met by either increasing the inhibitor potency toward *as* kinases or decreasing the potency toward *WT* kinases. The crystal structure of Hck–PP1 complex shows that the pyrazolopyrimidine ring of PP1 occupies the base-binding pocket within the kinase active site in a nearly identical manner to the adenine ring of ATP while the *p*-tolyl group at the 3-position projects from the pyrazolopyrimidine core into a deep hydrophobic pocket in the kinase active site (Fig. 1A).[11] The gatekeeper residue in Hck, T338, forms one side of this hydrophobic pocket and directly stacks on one face of the tolyl ring. The crystal structure reveals that the N^4 amino and the 3-tolyl groups of PP1 are in direct contact of T338. As one of its two N–H bonds points directly at T338, the N^4 position was first chosen for derivatization to generate allele-specific inhibitors. However, when N^4-substituted pyrazolopyrimidines were synthesized, it was found that due to a steric clash with the 3-tolyl group the N^4 substituent is forced into the cis conformation at the C4–N bond, which disrupted a key H-bond between PP1 and the kinase hinge region (Fig. 1A).[12] Subsequently, 3-position expanded analogs of PP1 were created to introduce a steric clash with the gatekeeper residue.[4] This effort succeeded in providing two pyrazolopyrimidine-based allele-specific kinase inhibitors, 1NA-PP1 and 1NM-PP1, which have been featured in the studies of various kinases. However, the extra moiety in these PP1 derivatives such as 1NA-PP1 is not oriented directly toward the gatekeeper and thus could only form a partial steric clash with T338 (Fig. 1A). It is conceivable that *WT* Hck could accommodate 1NA-PP1 through mild conformational reorganization, which may explain why 1NA-PP1 retains the ability to inhibit unmodified Src family kinases at micromolar concentrations (Table 1). The pyrazolopyrimidine scaffold dictates the relative orientation of the 3-substituent to the gatekeeper residue and makes it difficult to design PP1 derivatives with a more direct clash with the gatekeeper residue than 1NA-PP1.

We reasoned that inhibitors based on a different scaffold could possess greater selectivity with respect to *as* kinases if the scaffold could provide a platform for positioning substituents directly toward the gatekeeper residue while still maintaining unperturbed interactions with the hinge region. After examining the various protein kinase inhibitors reported in the literature, we selected the purine scaffold (exemplified by purvalanol) because it presents a distinct binding mode from PP1 and has potential to be derivatized to induce a direct steric clash with the gatekeeper residue.[13] Structural studies reveal that despite their isosteric structures purine and pyrazolopyrimidine are situated within the kinase active site with completely different orientations (Fig. 1). As a result, the frequently observed hydrogen bonds between

Table 1. IC_{50} values of 1NA-PP1, 1NM-PP1, and the purines **1–9** against CDK2 and v-Src kinases

Kinase	1NA-PP1	1NM-PP1	**1**	**2**	**3**	**4**	**5**	**6**	**7**	**8**	**9**
CDK2-as1	15 nM	5 nM	44 nM	300 nM	400 nM	7 μM	38 nM	60 nM	22 nM	20 nM	2 μM
CDK2-as2	ND	ND	1.5 μM	1 μM	1.3 μM	>100 μM	900 nM	700 nM	62 nM	940 nM	4 μM
CDK2-WT	18 μM	29 μM	7 μM	>100 μM	>100 μM	>100 μM	90 μM	>100 μM	>100 μM	>100 μM	>100 μM
v-Src-as1	1.5 nM	4 nM	42 nM	140 nM	500 nM	800 nM	11 nM	11 nM	11 nM	17 nM	180 nM
v-Src-as2	1 nM	15 nM	250 nM	360 nM	900 nM	14 μM	130 nM	140 nM	50 nM	150 nM	500 nM
v-Src-WT	1 μM	28 μM	>100 μM	>100 μM	>100 μM	>100 μM	>100 μM	>100 μM	>100 μM	>100 μM	>100 μM

'ND': not determined.

the inhibitor and the kinase hinge region were formed through a different set of atoms in a purvalanol analog (PVA) from PP1. The *m*-chlorophenyl group at N^6 of PVA projects outside the ATP binding pocket and contacts a loop region that is not exploited by PP1. The methyl group at N9, on the other hand, points directly at F80, the gatekeeper residue in CDK2. Based on this observation, we predicted that an enlarged N9-substituent on the purine scaffold would produce a direct steric clash with a bulky gatekeeper residue such as F80 in CDK2. Herein, we describe the synthesis of a series of 6,9-disubstituted purine derivatives and the evaluation of their inhibitory activity against a number of kinases in vitro and in vivo.

2. Results and discussion

We designed and synthesized a series of 6,9-disubstituted purines as specific inhibitors of analog-sensitized kinases. The substituents at the 6-position of the purines were fixed as a phenylamino group (considered a CDK specificity element, the *m*-chloro substituent on the phenyl ring was removed from PVA to maximize generality), while the N9-substituents were varied in the series to explore the gatekeeper pocket in *as* kinases (Schemes 1 and 2). In order to diminish their inhibitory activity against *WT* kinases, we designed the N9-substituents of these purines to be significantly larger than the corresponding groups (varying from Me to *i*-Pr) in the known purine-based kinase inhibitors (such as olomoucine and purvalanol) in order to produce a major steric clash with the gatekeeper residue in *WT* kinases (Fig. 1B).[14]

Several N9-alkyl purines (**1–4**) were synthesized in two steps using modified literature procedures (Scheme 1).[15] Reaction of 6-chloropurine with aniline in the first step afforded

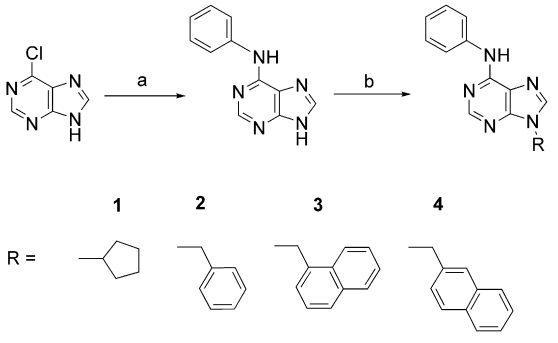

Scheme 1. (a) Aniline 2 equiv, *i*-PrOH, reflux, 1 h; (b) alkyl halide RX 1 equiv, K_2CO_3 1 equiv, DMF, rt, 1 h.

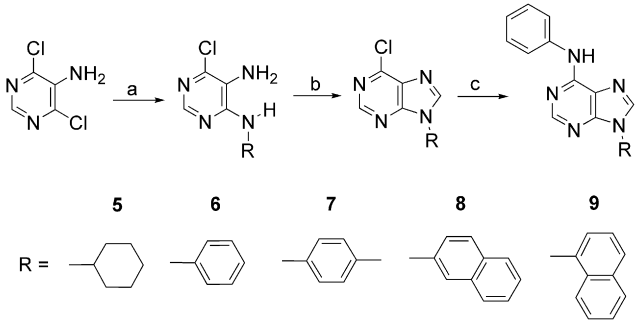

Scheme 2. (a) RNH_2 (R=cyclohexyl or aryl) 1 equiv, triethylamine 2 equiv, 1-butanol, reflux, 8 h; (b) triethylorthoformate 10 equiv, rt, 4 h; (c) aniline 2 equiv, *i*-PrOH, reflux, 1 h.

N^6-phenyladenine, which was subjected to reaction with different alkylating reagents in the second step to yield the respective N9-alkyl purines. The N9-cyclohexyl (**5**) and the N9-aryl purines (**6–9**) could not be produced using the above synthetic route because cyclohexyl bromide was found not reactive enough to alkylate N^6-phenyladenine and because no direct N9 arylation transformation is available. Analogs **5–9** were thus synthesized using a different route in three steps (Scheme 2).[16] 4,6-Dichloro-5-aminopyrimidine was reacted with cyclohexylamine or different arylamines, followed by treatment with triethylorthoformate to afford 6-chloro purines. Finally, reaction of the intermediates with aniline provided the desired 6,9-disubstituted purines (**5–9**).

We first examined the inhibitory activity of **1–9** against a serine/threonine kinase, cyclin-dependent kinase 2 (CDK2), and a tyrosine kinase v-Src by determining their IC_{50} values in vitro. Upon mutation of the gatekeeper residues (F80 in CDK2 and I338 in v-Src) to glycine (*as1* allele) or alanine (*as2* allele), CDK2 and v-Src were shown to be dramatically sensitized to the PP1 analogs such as 1NA-PP1 and 1NM-PP1 (Table 1).[5] The IC_{50} values of **1–9** against *WT* CDK2, CDK2-as1 ($CDK2^{F80G}$), and CDK2-as2 ($CDK2^{F80A}$) were determined. With the exception of **1**, all the purines in the series inhibit *WT* CDK2 poorly with IC_{50}s over 50 μM. In contrast, these compounds inhibit the glycine gatekeeper mutant CDK2-as1 potently with IC_{50}s in the nanomolar range, and the inhibitory selectivity toward CDK2-as1 over the *WT* is over 2000-fold for **5–8**. The alanine mutant, CDK2-as2, is inhibited by these purines at an intermediate level between the wild type and as1. When the inhibition of purines **1–9** against v-Src was measured, the IC_{50} values of all the purines in the series against *WT* v-Src were found to be over 100 μM (Table 1). In contrast, the IC_{50} values of **1–9** against the glycine mutant, v-Src-as1 ($v\text{-}Src^{I338G}$), lie in the nanomolar range with several compounds in the series (**5–7**)

approaching 10 nM. The purines **5**–**7** exhibit extraordinary inhibitory selectivity (>9000-fold) toward v-Src-as1 over the *WT*. Furthermore, these purines inhibit the alanine mutant, v-Src-as2 (v-Src^{I338A}), significantly less potently than v-Src-as1. This trend parallels that of CDK2, indicating that the purine derivatives are generally more effective inhibitors against the glycine gatekeeper mutant of a kinase than the alanine form.

A large number of chemical genetic studies of kinases have focused on the budding yeast *Saccharomyces cerevisiae* because of the relative ease of genetic manipulation and the fact that it is a single-cell eukaryote. As some of these purines are potent inhibitors of the *as1* allele of CDK2 and v-Src in vitro, we went on to examine their inhibition of Cdc28p, the budding yeast homolog of CDK2, in vivo. Being the major cyclin-dependent kinase in *S. cerevisiae*, Cdc28p shares high sequence homology (65% sequence identity) with the mammalian CDK2 and is essential for yeast viability.[17,18] We previously generated a mutant strain of *cdc28-as1* yeast by replacing *WT CDC28* with its *as1* allele (*cdc28-as1*).[5] Since the kinase activity of Cdc28p is essential for yeast viability, inhibitor candidates can be screened for inhibition of *cdc28-as1* using a halo assay.[19] A solution of each compound (**1**–**9**) was spotted onto a circular cellulose disk (0.6 cm diameter) laid on top of a yeast growth plate that is covered by an even lawn of yeast cells. Inhibition of *cdc28-as1* by the compound should prevent yeast growth near the cellulose disk, which results in the formation of a cell-free halo surrounding the disk.

When screened against the *cdc28-as1* yeast, several purines caused large halos indicating that they efficiently cross the yeast plasma membrane and inhibit Cdc28-as1 in the cell (Fig. 2). As the high sequence conservation between Cdc28p and CDK2 predicts, the most potent inhibitors in the purine series (**1**, **5**–**8**) against *cdc28-as1* in vivo turned out to be the same as the most potent compounds found for CDK2 in vitro (Table 1). These five compounds cause halos of comparable size to those by 1NM-PP1 (N in Fig. 2), the most effective PP1-derived inhibitor for *cdc28-as1*. Importantly, these purine derivatives produced no halo on the *WT* strain under the same conditions, discounting the possibility that they cause halos by inhibiting *WT* kinases or other yeast proteins (Fig. 2).

3. Conclusions

In an attempt to improve upon the selectivity of the PP1-derived inhibitors for *as* kinases we have examined a new kinase inhibitor scaffold for the development of more selective allele-specific kinase inhibitors in the current study. Aided by the crystal structure of CDK2–purvalanol complex, we designed and synthesized a series of 6,9-disubstituted purines as allele-specific kinase inhibitors. Several purines (**1**, **5**, **6**, and **7**) exhibit potent inhibitory activity against both CDK2-as1 and v-Src-as1 in vitro with low nanomolar IC_{50} values, which approach the potency of the most effective PP1 analogs such as 1NA-PP1 and 1NM-PP1. Most importantly, these purines poorly inhibit *WT* CDK2 and v-Src (IC_{50} >100 μM) and display high selectivity toward the *as1* allele over the *WT* kinase. These data support the conclusion that purine N9-substituents in these purines can indeed occupy the gatekeeper pocket as designed and contribute to the potency and selectivity of these purines toward *as* kinases.

We also investigated the in vivo inhibitory activity of these purine derivatives against the *as1* allele of an essential yeast kinase *CDC28* using a growth inhibition assay. Purines **1**, **5**–**8** caused halos to the *cdc28-as1* yeast indicating that these molecules can cross the yeast plasma membrane and inhibit the target kinase. Good membrane permeability is a property critical for the practical utility of small-molecule inhibitors in cell biology studies.[20]

While the purine derivatives exhibit improved inhibitory selectivity toward glycine-substituted kinases (*as1*), their potency does not exceed those of 1NA-PP1 and 1NM-PP1

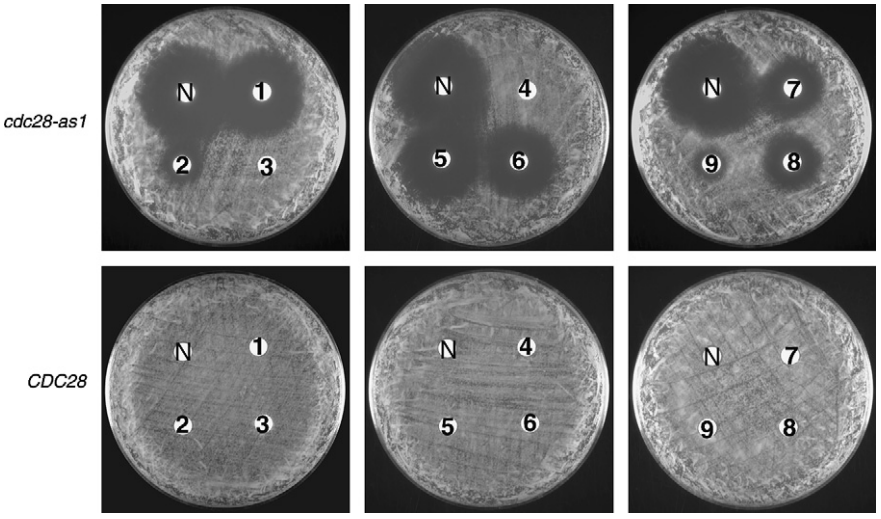

Figure 2. Compounds **1**–**9** were tested in the halo assay against the *cdc28-as1* yeast and the *CDC28* wild-type strain. 1NM-PP1 is included on each plate for comparison and is labeled as N on the plates. Several purines caused large halos to *cdc28-as1*, but not *CDC28* yeast. Approximately 2×10^5 cells were spread evenly on each plate before four circular cellulose disks (0.6 cm diameter) were gently laid on top of the plate. Ten microliters of each inhibitor solution (in DMSO at 2 mM) was subsequently added to one cellulose disk. The images of the plates were taken after 30-h incubation at 30 °C.

in the examples examined so far. The key advantage of the purine series, reported in this study, over the pyrazolopyrimidine series is the significant improvement in orthogonality with respect to *WT* kinases. Whereas the commonly used pyrazolopyrimidine inhibitor 1NA-PP1 has a selectivity factor [IC_{50}(*WT*)/IC_{50}(*as*)] of 700 for v-Src, purines **5–7** exhibit a selectivity factor over 10,000-fold. In addition, considering the small number and simplicity of the purines synthesized in the current study, there remain significant opportunities for improvement. Derivatization at C2 in the purine ring and further diversification of the substituents at N^6 and N9 will likely lead to improvements in potency.[13] The availability of a second series of allele-specific kinase inhibitors will provide additional chemical tools for interrogating the diverse kinases in the kinome.

4. Experimental

4.1. General

Materials obtained commercially were reagent grade and were used without further purification. ^{1}H NMR and ^{13}C NMR spectra were recorded on a Varian 400 spectrometer at 400 and 100 MHz, respectively. High-resolution electron impact mass spectra were recorded on a MicoMass VG70E spectrometer at the University of California-San Francisco center for Mass Spectrometry. Reactions were monitored by thin layer chromatography (TLC), using Merck silica gel 60 F_{254} glass plates (0.25 mm thick). Flash chromatography was conducted with Merck silica gel 60 (230–400 mesh).

4.2. General procedures for the synthesis of 1–4 exemplified by 1

4.2.1. N^6-Phenyladenine. A solution of 6-chloropurine (1.0 g, 6.5 mmol) and aniline (1.21 g, 13.0 mmol) in 50 mL isopropanol was refluxed for 2 h. The reaction mixture was added to 50 mL 1 M $NaHCO_3$ aqueous solution and extracted with ethyl acetate (3×60 mL). The extracts were combined and evaporated in vacuo to yield 1.17 g (85%) of yellowish product. The crude product was recrystalized from ethyl acetate to give 1.04 g (76%) of N^6-phenyladenine as colorless crystals; ^{1}H NMR (DMSO, 400 MHz) δ 7.01 (t, 1H, C*H*-4′), 7.31 (t, 2H, C*H*-3′), 7.95 (d, 2H, C*H*-2′), 8.27 (s, 1H, C*H*-2), 8.37 (s, 1H, C*H*-8), 9.72 (s, 1H, N*H*), 13.12 (s, 1H, N*H*-arom); ^{13}C NMR (DMSO, 100 MHz) δ 120.5 (*C*H-4′), 120.5 (*C*H-2′), 122.3 (*C*H-3′), 128.4 (*C*-5), 139.8 (*C*-arom), 139.8 (*C*-arom), 151.8 (*C*-arom), 151.8 (*C*-arom), 151.8 (*C*-arom); HRMS (EI) molecular ion calculated for $C_{11}H_9N_5$ 211.08580, found 211.08545.

4.2.2. (9-Cyclopentyl-9*H*-purin-6-yl)-phenylamine (1). A mixture of N^6-phenyladenine (0.70 g, 3.3 mmol), cyclopentyl iodide (0.65 g, 3.5 mmol), and K_2CO_3 (0.48 g, 3.5 mmol) in 20 mL of DMF was stirred overnight. The solvent was evaporated and the yellow residue was triturated with water and recrystalized from ethanol/water to yield 0.73 g (81%) of product. Colorless crystals; IR (thin film) 3327, 2964, 1622, 1582, 1498, 1476, 751, 646 cm^{-1}; ^{1}H NMR (DMSO, 400 MHz) δ 1.70 (m, 2H, C*H*-3″), 1.88 (m, 2H, C*H*-3″), 2.03 (m, 2H, C*H*-2″), 2.16 (m, 2H, C*H*-2″), 4.90 (m, 1H, C*H*-1″), 7.02 (t, *J*=8 Hz, 1H, C*H*-4′), 7.31 (t, *J*=8 Hz, 2H, C*H*-3′), 7.94 (d, *J*=8 Hz, 2H, C*H*-2′), 8.38 (s, 2H, C*H*-2,8), 9.80 (s, 1H, N*H*); ^{13}C NMR (DMSO, 100 MHz) δ 23.6 (*C*H_2-3″), 31.9 (*C*H_2-2″), 55.5 (*C*H-1″), 120.2 (*C*H-4′), 120.7 (*C*H-1′), 122.4 (*C*H-3′), 128.3 (*C*-5), 139.8 (*C*-6), 140.3 (*C*-1′), 149.6 (*C*H-8), 151.5 (*C*H-2), 152.0 (*C*-4); HRMS (EI) molecular ion calculated for $C_{16}H_{17}N_5$ 279.14840, found 279.14910.

4.2.3. (9-Benzyl-9*H*-purin-6-yl)-phenylamine (2). Colorless crystals; IR (thin film) 3052, 1624, 1579, 1497, 1477, 1232, 726, 695 cm^{-1}; ^{1}H NMR (DMSO, 400 MHz) δ 5.44 (s, 2H, CH_2), 7.02 (t, *J*=8 Hz, 1H, C*H*-4′), 7.31 (t, *J*=8 Hz, 2H, C*H*-arom), 7.33 (m, 5H, C*H*-arom), 7.94 (d, *J*=8 Hz, 2H, C*H*-arom), 8.40 (s, 1H, C*H*-2), 8.44 (s, 1H, C*H*-8), 9.87 (s, 1H, N*H*); ^{13}C NMR (DMSO, 100 MHz) δ 46.3 (*C*H_2), 119.7 (*C*-arom), 120.8 (*C*-arom), 122.5 (*C*-arom), 127.6 (*C*-arom), 127.8 (*C*-arom), 128.3 (*C*-arom), 128.7 (*C*-arom), 136.9 (*C*-arom), 139.7 (*C*-arom), 141.7 (*C*-arom), 149.6 (*C*H-8), 152.0 (*C*H-2), 152.1 (*C*-4); HRMS (EI) molecular ion calculated for $C_{18}H_{15}N_5$ 301.13275, found 301.13289.

4.2.4. (9-Naphthalen-1-ylmethyl-9*H*-purin-6-yl)-phenylamine (3). White powder; IR (thin film) 3050, 1621, 1581, 1498, 1476, 1232, 753, 692 cm^{-1}; ^{1}H NMR (DMSO, 400 MHz) δ 5.93 (s, 2H, CH_2), 7.03 (t, *J*=7 Hz, 1H, C*H*-4′), 7.24 (t, *J*=7 Hz, 1H, C*H*-arom), 7.32 (t, *J*=8 Hz, 2H, C*H*-arom), 7.47 (t, *J*=8 Hz, 1H, C*H*-arom), 7.58 (m, 2H, C*H*-arom), 7.94 (m, 4H, C*H*-arom), 8.28 (d, *J*=8 Hz, 1H, C*H*-arom), 8.35 (s, 1H, C*H*-2), 8.43 (s, 1H, C*H*-8), 9.90 (s, 1H, N*H*); ^{13}C NMR (DMSO, 100 MHz) δ 44.1 (*C*H_2), 119.6 (*C*-arom), 120.8 (*C*-arom), 122.6 (*C*-arom), 123.0 (*C*-arom), 125.6 (*C*-arom), 125.8 (*C*-arom), 126.2 (*C*-arom), 126.8 (*C*-arom), 128.3 (*C*-arom), 128.5 (*C*-arom), 128.7 (*C*-arom), 130.3 (*C*-arom), 132.3 (*C*-arom), 133.3 (*C*-arom), 139.6 (*C*-arom), 141.8 (*C*-arom), 149.8 (*C*H-8), 152.1 (*C*-arom), 152.1 (*C*-arom); HRMS (EI) molecular ion calculated for $C_{22}H_{17}N_5$ 351.14840, found 351.14841.

4.2.5. (9-Naphthalen-2-ylmethyl-9*H*-purin-6-yl)-phenylamine (4). White powder; IR (thin film) 3052, 1621, 1581, 1497, 1477, 1232, 751, 692 cm^{-1}; ^{1}H NMR (DMSO, 400 MHz) δ 5.61 (s, 2H, CH_2), 7.02 (t, *J*=8 Hz, 1H, C*H*-4′), 7.31 (t, *J*=8 Hz, 2H, C*H*-arom), 7.50 (m, 3H, C*H*-arom), 7.87 (m, 4H, C*H*-arom), 7.94 (d, *J*=8 Hz, 2H, C*H*-arom), 8.40 (s, 1H, C*H*-2), 8.49 (s, 1H, C*H*-8), 9.88 (s, 1H, N*H*); ^{13}C NMR (DMSO, 100 MHz) δ 46.5 (*C*H_2), 119.7 (*C*-arom), 120.7 (*C*-arom), 122.5 (*C*-arom), 125.6 (*C*-arom), 126.2 (*C*-arom), 126.2 (*C*-arom), 126.5 (*C*-arom), 127.6 (*C*-arom), 127.7 (*C*-arom), 128.3 (*C*-arom), 128.4 (*C*-arom), 132.4 (*C*-arom), 132.8 (*C*-arom), 134.4 (*C*-arom), 139.7 (*C*-arom), 141.8 (*C*-arom), 149.7 (*C*H-8), 152.0 (*C*-arom), 152.1 (*C*-arom); HRMS (EI) molecular ion calculated for $C_{22}H_{17}N_5$ 351.14840, found 351.14916.

4.3. General procedures for the synthesis of 5–9 exemplified by 5

4.3.1. 6-Chloro-9-cyclohexyl-9*H*-purine. A solution of 4,6-dichloropurine (1.64 g, 10.0 mmol), cyclohexylamine (0.99 g, 10.0 mmol), and triethylamine (2.02 g, 20.0 mmol) in 50 mL 1-butanol was refluxed. After 8 h, the solution was concentrated in vacuo to give a brown residue. This

intermediate product was added to triethylorthoformate and the solution was stirred at rt for 4 h. The solvent was evaporated and the yellow residue was recrystalized from ethyl acetate to yield 1.20 g (51%) of the product. Colorless crystals; ^{1}H NMR (DMSO, 400 MHz) δ 1.27 (m, 1H, C*H*-4′), 1.45 (m, 2H, C*H*-3′), 1.69 (br d, J=12 Hz, 1H, C*H*-4′), 1.86 (br d, J=14 Hz, 2H, C*H*-3′), 1.98 (m, 4H, CH_2-2′), 4.50 (m, 1H, C*H*-1′), 8.76 (s, 1H, C*H*-8), 8.79 (s, 1H, C*H*-2); HRMS (EI) molecular ion calculated for $C_{11}H_{13}N_4Cl$ 236.08287, found 236.08357.

4.3.2. (9-Cyclohexyl-9*H*-purin-6-yl)-phenylamine (5). A solution of 6-chloro-9-cyclohexyl-9*H*-purine (0.60 g, 2.5 mmol) and aniline (0.46 g, 5.0 mmol) in 30 mL isopropanol was refluxed for 2 h. The reaction mixture was added to 50 mL 1 M $NaHCO_3$ aqueous solution and extracted with ethyl acetate (3×60 mL). The extracts were combined and evaporated in vacuo to give a brown residue, which was further purified by column chromatography (5% Et_2O/$CHCl_3$) to yield 0.61 g (83%) of product. White powder; IR (thin film) 2934, 1622, 1582, 1497, 1475, 1233, 750, 646 cm^{-1}; ^{1}H NMR (DMSO, 400 MHz) δ 1.25 (m, 1H, C*H*-4″), 1.44 (m, 2H, C*H*-3″), 1.71 (br d, J=13 Hz, 1H, C*H*-4″), 1.86 (br d, J=14 Hz, 2H, C*H*-4″), 2.00 (m, 4H, CH_2-2″), 4.41 (m, 1H, C*H*-1″), 7.02 (t, J=8 Hz, 1H, C*H*-4′), 7.31 (t, J=8 Hz, 2H, C*H*-3′), 7.94 (d, J=8 Hz, 2H, C*H*-2′), 8.37 (s, 1H, C*H*-2), 8.39 (s, 1H, C*H*-8), 9.80 (s, 1H, N*H*); ^{13}C NMR (DMSO, 100 MHz) δ 24.8 (*C*-4″), 25.1 (*C*-3″), 32.3 (*C*-2″), 53.9 (*C*-1″), 120.7 (*C*-arom), 120.0 (*C*-arom), 122.5 (*C*-arom), 128.4 (*C*-arom), 139.8 (*C*-arom), 140.0 (*C*-arom), 149.2 (*C*H-8), 151.5 (*C*H-2), 152.0 (*C*-4); HRMS (EI) molecular ion calculated for $C_{17}H_{19}N_5$ 293.16405, found 293.16393.

4.3.3. Phenyl-(9-phenyl-9*H*-purin-6-yl)-amine (6). White powder; IR (thin film) 3048, 1623, 1584, 1500, 1475, 1373, 751, 691 cm^{-1}; ^{1}H NMR (DMSO, 400 MHz) δ 7.05 (t, J=8 Hz, 1H, C*H*-4′), 7.34 (t, J=8 Hz, 2H, C*H*-3′), 7.46 (t, J=8 Hz, 1H, C*H*-4″), 7.60 (t, J=8 Hz, 2H, C*H*-3″), 7.92 (d, J=8 Hz, 2H, C*H*-2′), 7.97 (d, J=8 Hz, 2H, C*H*-2″), 8.46 (s, 1H, C*H*-2), 8.76 (s, 1H, C*H*-8), 9.99 (s, 1H, N*H*); ^{13}C NMR (DMSO, 100 MHz) δ 120.3 (*C*-arom), 120.9 (*C*-arom), 122.8 (*C*-arom), 123.2 (*C*-arom), 127.7 (*C*-arom), 128.4 (*C*-arom), 129.5 (*C*-arom), 134.9 (*C*-arom), 139.6 (*C*-arom), 140.6 (*C*-arom), 149.3 (*C*H-8), 152.4 (*C*H-2), 152.6 (*C*-4); HRMS (EI) molecular ion calculated for $C_{17}H_{13}N_5$ 287.11710, found 287.11692.

4.3.4. Phenyl-(9-*p*-tolyl-9*H*-purin-6-yl)-amine (7). White powder; IR (thin film) 3048, 1623, 1585, 1516, 1497, 1475, 1373, 750 cm^{-1}; ^{1}H NMR (DMSO, 400 MHz) δ 2.38 (s, 3H, CH_3), 7.04 (t, J=8 Hz, 1H, C*H*-4′), 7.33 (t, J=8 Hz, 2H, C*H*-3′), 7.39 (d, J=8 Hz, 2H, C*H*-3″), 7.78 (d, J=8 Hz, 2H, C*H*-2′), 7.97 (d, J=8 Hz, 2H, C*H*-2″), 8.44 (s, 1H, C*H*-2), 8.71 (s, 1H, C*H*-8), 9.97 (s, 1H, N*H*); ^{13}C NMR (DMSO, 100 MHz) δ 20.6 (*C*H$_3$), 120.3 (*C*-arom), 120.9 (*C*-arom), 122.7 (*C*-arom), 123.0 (*C*-arom), 128.4 (*C*-arom), 129.9 (*C*-arom), 132.4 (*C*-arom), 137.2 (*C*-arom), 139.6 (*C*-arom), 140.6 (*C*-arom), 149.3 (*C*H-8), 152.3 (*C*H-2), 152.5 (*C*-4); HRMS (EI) molecular ion calculated for $C_{18}H_{15}N_5$ 301.13275, found 301.13294.

4.3.5. (9-Naphthalen-2-yl-9*H*-purin-6-yl)-phenylamine (8). White powder; IR (thin film) 1619, 1583, 1497, 1477, 1376, 1180, 748, 691 cm^{-1}; ^{1}H NMR (DMSO, 400 MHz) δ 7.06 (t, J=8 Hz, 1H, C*H*-4′), 7.35 (t, J=8 Hz, 2H, C*H*-3′), 7.62 (m, 2H, C*H*-arom), 7.99 (d, J=8 Hz, 2H, C*H*-2′), 8.04 (d, J=8 Hz, 2H, C*H*-arom), 8.10 (dd, J_1=9 Hz, J_2=2 Hz, 1H, C*H*-arom), 8.17 (d, J=9 Hz, 1H, C*H*-arom), 8.51 (s, 2H, C*H*-2), 8.90 (s, 1H, C*H*-8), 10.03 (s, 1H, N*H*); ^{13}C NMR (DMSO, 100 MHz) δ 120.4 (*C*-arom), 120.9 (*C*-arom), 121.0 (*C*-arom), 121.7 (*C*-arom), 122.8 (*C*-arom), 126.7 (*C*-arom), 127.2 (*C*-arom), 127.8 (*C*-arom), 128.0 (*C*-arom), 128.5 (*C*-arom), 129.4 (*C*-arom), 131.8 (*C*-arom), 132.5 (*C*-arom), 133.0 (*C*-arom), 139.6 (*C*-arom), 140.8 (*C*-arom), 149.5 (*C*H-8), 152.4 (*C*H-2), 152.7 (*C*-4); HRMS (EI) molecular ion calculated for $C_{21}H_{15}N_5$ 337.13275, found 337.13166.

4.3.6. (9-Naphthalen-1-yl-9*H*-purin-6-yl)-phenylamine (9). White powder; ^{1}H NMR (DMSO, 400 MHz) δ 7.06 (t, J=7 Hz, 1H, C*H*-4′), 7.34 (m, 3H, C*H*-arom), 7.54 (t, J=7 Hz, 1H, C*H*-arom), 7.64 (t, J=7 Hz, 1H, C*H*-arom), 7.72 (m, 2H, C*H*-arom), 7.99 (d, J=8 Hz, 2H, C*H*-2′), 8.13 (d, J=8 Hz, 1H, C*H*-arom), 8.19 (d, J=8 Hz, 1H, C*H*-arom), 8.31 (s, 1H, C*H*-2), 8.61 (s, 1H, C*H*-8), 10.07 (s, 1H, N*H*); ^{13}C NMR (DMSO, 100 MHz) δ 119.5 (*C*-arom), 121.0 (*C*-arom), 122.4 (*C*-arom), 122.7 (*C*-arom), 125.6 (*C*-arom), 125.9 (*C*-arom), 126.9 (*C*-arom), 127.6 (*C*-arom), 128.3 (*C*-arom), 128.4 (*C*-arom), 129.4 (*C*-arom), 129.7 (*C*-arom), 130.7 (*C*-arom), 133.7 (*C*-arom), 139.6 (*C*-arom), 142.5 (*C*-arom), 151.2 (*C*H-8), 152.4 (*C*H-2), 152.6 (*C*-4); HRMS (EI) molecular ion calculated for $C_{21}H_{15}N_5$ 337.13275, found 337.13349.

4.4. Kinase inhibition assays in vitro

Glutathione *S*-transferase (GST) fused v-Src proteins were expressed in *Escherichia coli* and purified on glutathione beads as described previously.[4] In the v-Src kinase assay, various concentrations of inhibitor were incubated with 50 mM Tris (pH 8.0), 10 mM $MgCl_2$, 1.6 mM glutathione, 1 mg/mL BSA, 0.1 mg/mL peptide substrate (IY-GEFKKK), 3.3% DMSO, and 11 nM (2 μCi) [γ-^{32}P]ATP (6000 Ci/mmol, NEN), and v-Src kinase in a total volume of 30 μL for 30 min. Reaction mixtures (27 μL) were spotted onto a phosphocellulose disk, and washed with 0.5% H_3PO_4. The transfer of ^{32}P was measured by standard scintillation counting. IC_{50} values were defined to be the concentration of inhibitor at which the radioactivity counts remaining on the phosphocellulose disk were inhibited by 50%.

6×His tagged CDK2 and cyclin E were expressed in SF9 cells and purified on Ni-NTA beads as described previously.[5] In the CDK2 kinase assay, various concentrations of inhibitor were incubated with 20 mM Tris (pH 7.4), 100 mM NaCl, 10 mM $MgCl_2$, 1 mg/mL BSA, 0.1 mg/mL peptide substrate (RGGKSPRKGNSSKKK), 3.3% DMSO, and 11 nM (2 μCi) [γ-^{32}P]ATP (6000 Ci/mmol, NEN), and CDK2/ClnE complex in a total volume of 30 μL for 30 min. The other procedures of the CDK2 kinase assay are the same as those of the v-Src assay.

4.5. Halo assay for *cdc28-as1* inhibition

The *cdc28-as1* yeast was created as previously described.[5] Approximately 2×10^5 cells isolated during log phase growth

($OD_{660} \approx 0.5$) in liquid YPD were spread evenly on each plate before four circular cellulose disks (0.6 cm diameter) were gently laid on top of the plate. 10 μL of each inhibitor solution (in DMSO at 2 mM) was subsequently added to one cellulose disk. The images of the plates were taken on an Alpha Innotech Imaging Center after 30-h incubation at 30 °C.

Acknowledgements

We thank J. D. Blethrow for kindly providing the CDK2 proteins and NIH for funding (AI44009).

References and notes

1. Lee, J. C.; Laydon, J. T.; McDonnell, P. C.; Gallagher, T. F.; Kumar, S.; Green, D.; McNulty, D.; Blumenthal, M. J.; Heys, J. R.; Landvatter, S. W.; Strickler, J. E.; McLaughlin, M. M.; Siemens, I. R.; Fisher, S. M.; Livi, G. P.; White, J. R.; Adams, J. L.; Young, P. R. *Nature* **1994**, *372*, 739–746.
2. Davies, S. P.; Reddy, H.; Caivano, M.; Cohen, P. *Biochem. J.* **2000**, *351*, 95–105.
3. Fabian, M. A.; Biggs, W. H., 3rd; Treiber, D. K.; Atteridge, C. E.; Azimioara, M. D.; Benedetti, M. G.; Carter, T. A.; Ciceri, P.; Edeen, P. T.; Floyd, M.; Ford, J. M.; Galvin, M.; Gerlach, J. L.; Grotzfeld, R. M.; Herrgard, S.; Insko, D. E.; Insko, M. A.; Lai, A. G.; Lelias, J. M.; Mehta, S. A.; Milanov, Z. V.; Velasco, A. M.; Wodicka, L. M.; Patel, H. K.; Zarrinkar, P. P.; Lockhart, D. J. *Nat. Biotechnol.* **2005**, *23*, 329–336.
4. Bishop, A.; Kung, C.; Shah, K.; Witucki, L.; Shokat, K.; Liu, Y. *J. Am. Chem. Soc.* **1999**, *121*, 627–631.
5. Bishop, A. C.; Ubersax, J. A.; Petsch, D. T.; Matheos, D. P.; Gray, N. S.; Blethrow, J.; Shimizu, E.; Tsien, J. Z.; Schultz, P. G.; Rose, M. D.; Wood, J. L.; Morgan, D. O.; Shokat, K. M. *Nature* **2000**, *407*, 395–401.
6. Adams, J.; Huang, P.; Patrick, D. *Curr. Opin. Chem. Biol.* **2002**, *6*, 486–492.
7. Zhang, C.; Kenski, D. M.; Paulson, J. L.; Bonshtien, A.; Sessa, G.; Cross, J. V.; Templeton, D. J.; Shokat, K. M. *Nat. Methods* **2005**, *2*, 435–441.
8. Chen, X.; Ye, H.; Kuruvilla, R.; Ramanan, N.; Scangos, K. W.; Zhang, C.; Johnson, N. M.; England, P. M.; Shokat, K. M.; Ginty, D. D. *Neuron* **2005**, *46*, 13–21.
9. Ventura, J. J.; Hubner, A.; Zhang, C.; Flavell, R. A.; Shokat, K. M.; Davis, R. J. *Mol. Cells* **2006**, *21*, 701–710.
10. Hanke, J. H.; Gardner, J. P.; Dow, R. L.; Changelian, P. S.; Brissette, W. H.; Weringer, E. J.; Pollok, B. A.; Connelly, P. A. *J. Biol. Chem.* **1996**, *271*, 695–701.
11. Schindler, T.; Sicheri, F.; Pico, A.; Gazit, A.; Levitzki, A.; Kuriyan, J. *Mol. Cells* **1999**, *3*, 639–648.
12. Bishop, A. C.; Shah, K.; Liu, Y.; Witucki, L.; Kung, C.; Shokat, K. M. *Curr. Biol.* **1998**, *8*, 257–266.
13. Gray, N. S.; Wodicka, L.; Thunnissen, A. M.; Norman, T. C.; Kwon, S.; Espinoza, F. H.; Morgan, D. O.; Barnes, G.; LeClerc, S.; Meijer, L.; Kim, S. H.; Lockhart, D. J.; Schultz, P. G. *Science* **1998**, *281*, 533–538.
14. Haesslein, J. L.; Jullian, N. *Curr. Top. Med. Chem.* **2002**, *2*, 1037–1050.
15. Reitz, A.; Graden, D.; Jordan, A.; Maryanoff, B. *J. Org. Chem.* **1990**, *55*, 5761–5766.
16. Thompson, R.; Secunda, S.; Daly, J.; Olsson, R. *J. Med. Chem.* **1991**, *34*, 2877–2882.
17. Morgan, D. O. *Annu. Rev. Cell Dev. Biol.* **1997**, *13*, 261–291.
18. Mendenhall, M. D.; Hodge, A. E. *Microbiol. Mol. Biol. Rev.* **1998**, *62*, 1191–1243.
19. Manney, T. R. *J. Bacteriol.* **1983**, *155*, 291–301.
20. Rogers, B.; Decottignies, A.; Kolaczkowski, M.; Carvajal, E.; Balzi, E.; Goffeau, A. *J. Mol. Microbiol. Biotechnol.* **2001**, *3*, 207–214.